

Wind observations from a forested hill: Relating turbulence statistics to surface characteristics in hilly and patchy terrain

LUKAS PAUSCHER^{1,2*}, DORON CALLIES¹, TOBIAS KLAAS¹ and THOMAS FOKEN²

¹Fraunhofer Institute for Wind Energy and Energy System Technology IWES, Kassel, Germany

²Department of Micrometeorology University of Bayreuth, Bayreuth Center of Ecology and Environmental Research, Bayreuth, Germany

(Manuscript received April 17, 2017; in revised form August 7, 2017; accepted August 9, 2017)

Abstract

This study investigates turbulence characteristics as observed at a 200 m tall mast at a hilly and complex site. It thereby concentrates on turbulence statistics, which are important for the site suitability analysis of a wind turbine. The directional variations in terrain are clearly reflected in the observed turbulence intensities and drag. Integral turbulence statistics showed some variations from their typical flat terrain values. Footprint modelling was used to model the area of effect and to relate the observed turbulence characteristics to the ruggedness and roughness within the estimated fetch area. Among the investigated turbulence quantities, the normalised standard deviation of the wind velocity along the streamlines showed the highest correlation with the effective roughness and ruggedness within the footprint followed by the normalised friction velocity and normalised standard deviation of the vertical wind speed. A differentiation between the effects of roughness and ruggedness was not possible, as forest cover and complex orography are highly correlated at the investigated site. An analysis of turbulence intensity by wind speed indicated a strong influence of atmospheric stability. Stable conditions lead to an overall reduction in turbulence intensity for a wind speed range between approx. 6–12 m s⁻¹ when compared to neutral stratification. The variance of the horizontal wind speed strongly varied over the height range which is typical for a modern wind turbine and was in the order of the differences between different standard turbulence classes for wind turbines.

Keywords: wind energy, turbulence intensity, footprint, complex terrain, ruggedness, design wind conditions

1 Introduction

Today a significant part of the wind energy development in, e.g., Germany takes place at inland sites located relatively far from the coast (BERKHOUT *et al.*, 2015). New turbine technology has made sites with relatively low wind speeds and/or forest cover technically and economically viable. Due to the increased wind resource, hilltop locations in lower mountain ranges are attractive for turbine siting in this context. This results in a significant increase in complexity of orography of the terrain when compared to many coastal sites, where a lot of the wind energy development has taken place in the past. Also, a lot of the unused wind energy potential of e.g. Germany and Scandinavia is located in complex and/or forested terrain (CALLIES, 2015; SIYAL *et al.*, 2015). Many of these potential sites exhibit a significant amount of heterogeneity in surface cover and orography.

To avoid the increased turbulence induced by forest canopies and to make use of the larger wind resources at greater heights, modern wind turbines at inland sites now reach hub heights of 160 m and more. The tip heights of modern wind turbines can reach

well above 200 m. Despite this development there is very little published experimental wind and turbulence data from forested areas covering the height range relevant for wind energy applications. This is especially true when the effects of complex orography and patchy forested landscape are combined. As a consequence, there is a lack of validation of models used in wind resource estimation and site assessment in complex and patchy terrain. Therefore, the estimation of the wind resource and especially the turbulence parameters, which are required for the site suitability analysis of a wind turbine, are associated with high uncertainties.

The interest in ecosystem-atmosphere exchange of trace gases such as carbon dioxide has led to an extensive body of experimental studies of flows within and directly above plant canopies including complex and heterogeneous sites (e.g. BALDOCCHI, 2014). The vertical extension of measurements in these studies is often limited to twice of the canopy height. Therefore, most of these experimental results only have limited value in the context of wind energy applications. One of the few sites with published experimental results from a tall tower (135 m) stems from a boreal forest in Sweden (ARNQVIST *et al.*, 2015). The analysis showed a general applicability of Monin-Obukhov similarity theory (MOST) with a slight deviation for upper heights, but also indicated the influence of a limited boundary

*Corresponding author: Lukas Pauscher, Fraunhofer Institute for Wind Energy and Energy System Technology IWES, Koenigstor 59, Kassel, Germany, e-mail: lukas.pauscher@iwes.fraunhofer.de

layer height on the wind profile. Additionally, a detailed analysis of turbulence statistics was presented. For the same site, [CHOUGULE et al. \(2015\)](#) investigated the turbulence spectra in the frame work of the spectral tensor model of [MANN \(1994\)](#) in near neutral conditions. As expected, they found strongly increased turbulence levels but could not observe significant differences in the length scales or anisotropy of the turbulence when compared to flat terrain. Both studies focused on a homogeneous wind sector.

If we turn our attention to the combination of orography and forested landscape, the lack of experimental data is even more severe and only a handful of published experimental field campaigns exist. As for forest in flat terrain, many studies in complex terrain only employ relatively short masts and thus are not suitable to investigate wind and turbulence statistics at elevated heights (e.g. [ZERI et al., 2010](#); [GRANT et al., 2015](#)). [BRADLEY \(1980\)](#) published measured wind and turbulence profiles for neutral conditions from a measurement tower up to 124 m over a 10 m tall eucalyptus forest and heterogeneous fetch conditions. A limited number of experimental results on the effects of orography covered by plant canopies is also available from wind tunnel experiments (e.g. [KAIMAL and FINNIGAN, 1994](#); [NEFF and MERONEY, 1998](#); [RUCK and ADAMS, 1991](#)) and flume experiments ([POGGI and KATUL, 2007](#); [POGGI and KATUL, 2008](#)). Besides the experimental evidence gathered, theoretical modelling studies have had a strong contribution to our current knowledge of flow over forested hills (e.g. [FINNIGAN and BELCHER, 2004](#); [ALLEN and BROWN, 2002](#); [BROWN et al., 2001](#); [ROSS and VOSPER, 2005](#); [PATTON and KATUL, 2009](#)).

Although modelling studies have started to turn on more complex inhomogeneous forests (e.g. [SOGACHEV et al., 2009](#); [BOUDREAULT, 2015](#)), it is still very difficult for the experimentalist or practitioner from the wind energy community to relate the observed wind and turbulence statistics to the surface characteristics surrounding the site in heterogeneous landscapes. Detailed models often require large computer resources as well as detailed expert knowledge and are thus not a feasible option in many situations. Recently, remotely-piloted aircraft have been used to experimentally explore small scale variations in the turbulent flow over complex orography in a wind energy context ([WILDMANN et al., 2017](#)).

In this paper we present turbulence and wind speed measurements from a 200 m tall tower located on a forested hill surrounded by a patchy and hilly landscape in central Germany. To analyse the link between the upstream surface characteristics and turbulence quantities, we borrow from the surface flux community and use footprint modelling (for an overview see e.g. [VESALA et al., 2008](#) or [LECLERC and FOKEN, 2014](#)) to identify the area influencing the measurement. We thus follow an idea which was recently suggested by [FOKEN \(2013\)](#) and experimentally investigate the transferability of the footprint approach to wind energy applications. Thereby,

this analysis mainly focuses on turbulence quantities which are relevant for the site suitability assessment of a wind turbine. The influence of surface cover is described using the classical concept of surface roughness, while the effects of orography are conceptualised using a ruggedness index. Also, the paper discusses some of the observations made at Rödeser Berg in relation to standards for the description of the turbulence environment ([IEC, 2005a](#)).

2 Methods

2.1 Experimental site and instrumentation

The data analysed in this paper was collected at a 200 m tall mast at Rödeser Berg in northern Hesse in Germany (51° 21' 46'' N, 9° 11' 43'' E). A brief description of the site can also be found in [KLAAS et al. \(2015\)](#) and [PAUSCHER et al. \(2016\)](#). The mast is located at the southwestern edge of a clearing (approx. 280 m north to south and 200 m east to west) on the ridge of a forested hill which stretches from approx. SSE to NNW (Figure 1).

The closer surroundings of the mast are characterised by forest of varying heights and several clearings. The distance, up to which the forests stretches, strongly varies with direction. In the direction NNW the forest extends approx. 5.8 km, while in ENE the forest edge is already reached within approx. 400 m from the mast. The orography of the hill also varies strongly with direction. In general, the terrain is hilly and undulated. Towards the NNW-direction a hilly ridge extends for about 5.8 km.

The wider surroundings consist of a patchy landscape of mainly agricultural land use, forest and some settlements. The immediate surroundings of the forested hill are mainly characterised by open agricultural areas. In the east and the west these are bordered by forested hills. In general, the terrain surrounding Rödeser Berg is very heterogeneous, which makes a definition of sectors with a consistent fetch as done in many other studies difficult if not impossible.

The mast consists of a rectangular lattice structure with a side length of 1.05 m. The solidity of the mast structure is $0.220 \text{ m}^2 \text{ m}^{-2}$ for the lower section (below 100 m) and $0.204 \text{ m}^2 \text{ m}^{-2}$ for the upper section (above 100 m). Here, solidity is defined according to [IEC \(2005b\)](#) as the projected area of all structural members divided by the exposed area of the mast. The mast is equipped with a dense array of sensors. An overview of the sensors used for the analysis is given in Table 1. Although the mast has opposing boom pairs, sonic anemometers are only mounted on the side facing 315–322°. The analysis in this paper thus focuses on the analysis of sensors mounted on this side. Since the mast structure is slightly twisting with height, boom directions vary with height. To minimise the effects of the mast structure, the wind sensors are mounted on booms with a length of 5.4 m and meet the recommendations

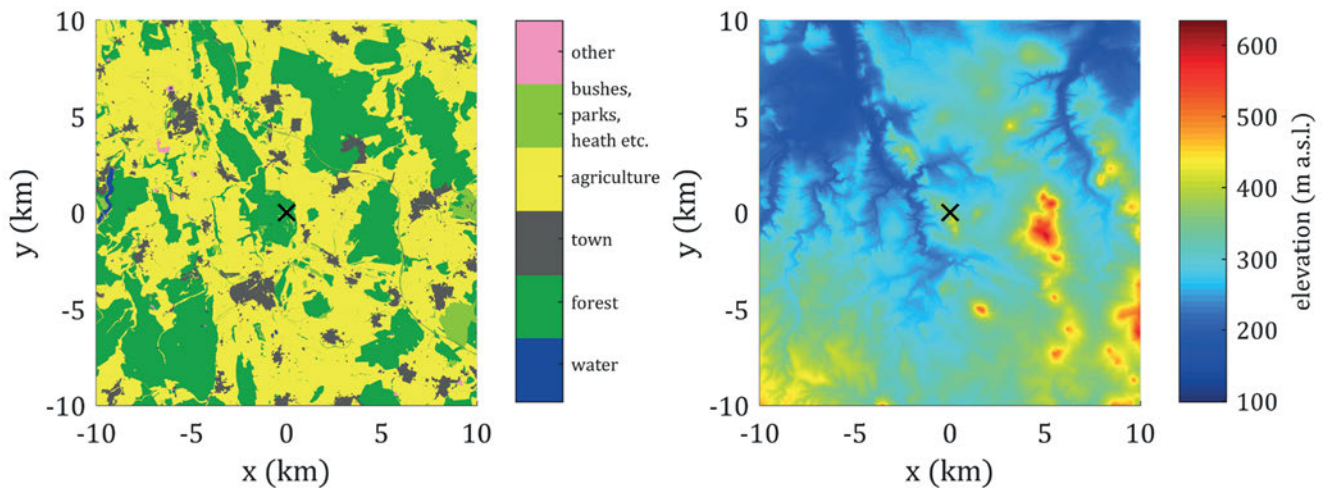


Figure 1: Left: Landuse map of the area around Rödeser Berg (data source ©GeoBasis-DE / Bundesamt für Kartographie und Geodäsie (2013) and www.openstreetmap.org); right: map of the terrain elevation around Rödeser Berg (data source ©GeoBasis-DE / Bundesamt für Kartographie und Geodäsie (2013)). The coordinate system for both maps is centered at the mast location – i.e. the location of the mast is (0,0).

Table 1: Overview of the anemometers used in this study; heights marked with* are bearing heated; heights marked with† are fully heated.

Sensor Type	height (m)	sampling frequency (Hz)	wind components
Thies First Class Advanced Cup Anemometer	60*, 120*, 191	1	U
Thies Ultrasonic Anemometer 3D	80†	20	u, v, w
Gill HS50 Ultrasonic Anemometer	40, 135, 188	50	u, v, w

given in (IEC, 2005b). The sector 100–180° is removed from the analysis to avoid mast shadow effects. This choice was made by looking at the wind speed ratio between two opposing cup anemometers at the height of 191 m. The interval was then chosen conservatively and a ‘safety band’ of 20° was put around the sector where the mast shadow effect was visible.

2.2 Data preparation and quality control

The data analysed in this study comprises a period between 01.07.2012 and 01.12.2014. After that, several wind turbines were installed on site and large sectors are now influenced by wind turbine wakes. The data was filtered for physically unreasonable values and spiky periods in the sonic anemometer measurements were removed from the analysis. All analysis is based on 10-minute intervals, as these are most commonly used in wind energy applications.

The wind speed measurements from the sonic anemometer are rotated into the mean stream lines for each individual period (KAIMAL and FINNIGAN, 1994) before calculation of turbulence statistics from the sonic data. Compared to the often used planar-fit method (WILCZAK et al., 2001), the double rotation has been suggested to be superior at complex sites with varying slopes (STIPERSKI and ROTACH, 2016). Due to multiple instrument defects of the sonic anemometers, however, the number of valid measurements and the periods for which the instruments were functional vary with height. Only averaging peri-

ods, when no data was missing during the averaging interval, were used. Complete profiles with measurements at all levels are indicated in the text or the caption of the figure/table.

In Section 3, three different normalisations are used to present the measured turbulence statistics. First results are presented in the classical micro-meteorological framework (Section 3.1). Here, the turbulence statistics are normalised by the local (measured at the same height) wind speed and friction velocity. This facilitates the comparison to other measurements in the literature. A normalisation with the surface value, i.e. the friction velocity at the lowest measurement height, does not seem to be reasonable due to the strong variations in the fetch area with height.

In Section 3.2, the presented turbulence statistics are normalised by the wind speed measured by the cup anemometer at 191 m. The aim of this section is the investigation of the relationship between the surface characteristics and the turbulence statistics. To avoid speed-up effects in the wind profile to bias this analysis a common wind speed for the normalisation is necessary here. Ideally, the normalisation would be done with a wind speed which is independent of the local surface characteristics (e.g. the geostrophic wind speed). However, this would involve additional modelling which introduces additional uncertainties. The wind speed measured by the cup at 191 m was chosen as it is furthest from the surface and speed-up effects due to the terrain are expected to be weaker than at the lower heights.

In Section 3.3, the turbulence statistics are investigated from the ‘perspective’ of a wind turbine. Therefore, the normalisation is made using the wind speed at 120 m (U_{120}), a typical current hub height. This also allows the evaluation of the variation of the variance in the wind field across the rotor area of a turbine – i.e. how much the variance of the wind field changes with height. The top (191 m) and bottom (60 m) heights in this analysis roughly correspond to these upper and lower tip heights. This means that turbulence intensities in Sections 3.1/3.2 and 3.3 are collected using different instruments and are expected to differ because of the different measurement principles of sonic and cup anemometers. This is also reflected in the taxonomy used in this article. The turbulence intensity derived from the cup anemometers is denoted by I_U to indicate that there is no directional information available. In contrast, the turbulence intensity of the sonics is denoted by I_u to indicate the vector component along the mean stream lines. In general, the cup anemometers are expected to yield slightly lower values for the turbulence intensities of the horizontal component because of their distance constant of 3–3.9 m and their averaging time of 1 s. The data from the cup anemometers in Section 3.3 is chosen for two reasons. Firstly, they had a higher availability than the sonic anemometers. Secondly, cup measurements at a sampling frequency of 1 Hz still provide the standard for the wind energy community, which is important if the measured data is compared to existing standards.

The focus of Sections 3.1 and 3.2 is put on the influence of the terrain on the variations in turbulence statistics. Therefore, only neutral conditions are considered in these sections.

2.3 Footprint analysis

Interpretation and understanding of observed wind and turbulence characteristics in a complex and heterogeneous environment like the current site pose a particular challenge to experimentalists. If the observations are to be linked to the surrounding surface/terrain, two major challenges need to be addressed. The surface area influencing the measurement (i.e. the area of effect) must be identified and appropriate measures for the characterisation of the surface/terrain within this area need to be found.

For the first problem in this study, a footprint modelling approach is used. Within the flux measurement community this method is widely used to relate observed scalar fluxes to source areas, which are seen by the sensor (RANNIK et al., 2012). Here, the footprint model of KLJUN et al. (2015), which is parametrised based on a more complex Langrian backward footprint model (KLJUN et al., 2002), is used to identify the surface area which is seen by the measurements at the different heights. The analysis then concentrates on the surface cover and the orography within the modelled footprint. The KLJUN et al. (2015) model is probably

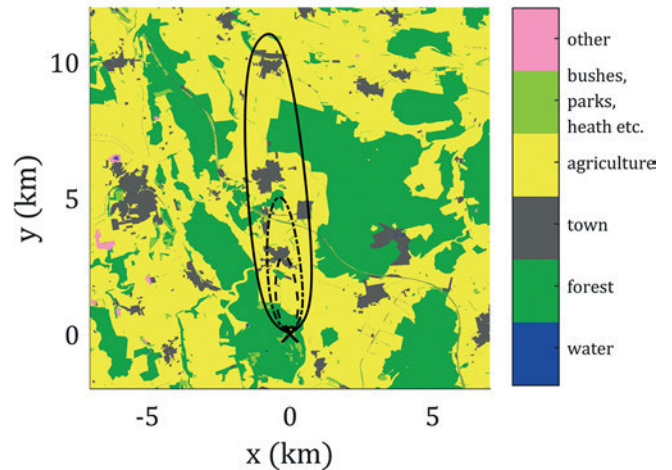


Figure 2: Example for a footprint climatology calculated for 135 m for neutral conditions and wind directions between 350–360°; the dashed, dash-dotted and solid lines indicate the 40-, 60- and 80%-effect levels of the flux footprint (data source ©GeoBasis-DE / Bundesamt für Kartographie und Geodäsie (2013) and www.openstreetmap.org).

nowadays the best easy-to-use model on a good theoretical basis. This model compared well with a LES footprint model (STEINFELD et al., 2008). It thus provides a good compromise between simplicity and functionality. While the input parameters are easily derived from sonic anemometer measurements it is still valid for a wide range of atmospheric conditions and elevated measurement heights. MARKKANEN et al. (2009) found that at heights of 100–200 m there is a good agreement between the KLJUN et al. (2002) model and a large eddy simulation for idealised conditions. A sample footprint climatology for a 10° sector is shown in Figure 2.

The analysis in this study is confined to neutral conditions. Therefore, the boundary layer height z_i in the footprint model can be approximated as

$$z_i = c_n \frac{u_*}{|f|}, \quad (2.1)$$

as recommended in the appendix by KLJUN et al. (2015). In Equation 2.1 u_* is the friction velocity, f is the Coriolis parameter and $c_n = 0.3$ (HANNA and CHANG, 1993). Periods where the estimate z_i was smaller than the measurement height (i.e. very small local friction velocities) were not considered in the footprint analysis. According to MARKKANEN et al. (2009), for z_i of about 500 m the footprint can be well determined for heights of about 200 m and less without a significant influence of the boundary layer height. Due to the wind speed limit (4 m s^{-1}), which was used, this applies to about 94 % of all measurement periods for the highest sonic anemometer. The influence of z_i on the footprint modelling results is, thus, expected to be small.

While strictly only valid for scalar fluxes, in this analysis the footprint approach is also used to identify the area which influences the measured turbulence statistics. The argument for the appropriateness of this

approach is derived from the fact that the vertical length scales of the footprint concept and the blending height concept as well as the internal boundary-layer concept are very similar (HORST, 2000). Moreover, following PHILIP (1997), a convection-diffusion equation for shear stress in analogy to passive scalars can be derived. If the eddy diffusivity and eddy viscosity are assumed to be equal, the blending height of scalar fluxes and shear stress are very similar.

In practical applications, FOKEN and LECLERC (2004) have suggested to use roughness changes and isolated obstacles as natural tracers to validate footprint models. Footprint models have also been used to estimate the averaged roughness representative of the footprint area of a measurement (GÖCKEDE et al., 2004; GÖCKEDE et al., 2006). More recently, the footprint approach has also been suggested to be used to estimate the area and, hence, the surface roughness influencing the wind conditions experienced by a wind turbine (FOKEN, 2013).

It should be noted, that the applied footprint model assumes homogeneous conditions and is thus not suited for heterogeneous terrain/flow. This is somewhat in contrast to the idea of identifying the relevant features in a heterogeneous environment, but is inherent in most footprint models. One of the purposes of this paper is to experimentally explore the applicability and limitations of the simplified footprint-modelling approach. Therefore, the footprint approach used in this study can only serve as a first approximation of the area of effect for a measurement/wind turbine. More sophisticated footprint models based on e.g. large eddy simulations (e.g. STEINFELD et al., 2008) might lead to more realistic results. However, this strongly increases the complexity of the model and therefore removes one of the main advantages of the footprint approach.

2.4 Terrain classification

For wind energy applications mainly the aerodynamic properties of the surface are of interest. These are strongly influenced by the surface cover and the drag which is exerted by the surface form or ruggedness of the terrain. The first aspect can be addressed by aggregating the roughness of the different land cover types into a roughness which is representative of the area of effect – i.e. the effective roughness length $z_{0,\text{eff}}$.

Here, the logarithmic average (TAYLOR, 1987) of the footprint weighted roughness length within the 80%-effect level of the footprint is used to determine $z_{0,\text{eff}}$:

$$\log(z_{0,\text{eff}}) = \sum_{i=1}^n p_i \log(z_{0,i}), \quad (2.2)$$

where p_i and $z_{0,i}$ are the footprint weighting and the roughness length assigned to each individual pixel; n is the number of pixels within the footprint.

It is acknowledged that there are more sophisticated averaging schemes available which also take the spatial

Table 2: Roughness lengths (z_0) for different surface cover types as used in this study (slightly modified after FOKEN, 2017).

Land cover	z_0 (m)
forest	1
settlements	1
agriculture, sports and recreational	0.03
bushes, clearings, swamps	0.2
gravel pit, waste disposal site	0.3
water	0.0005

arrangement of the different surface types within the averaging area into account (e.g. HASAGER and JENSEN, 1999; HASAGER et al., 2003). However, for simplicity reasons the simple logarithmic approach is chosen here. Also, it can often be used as a good first approximation (TAYLOR, 1987).

The surface cover and, thus, the underlying roughness map is based on a digital land-use model with a resolution of 10 m (Figure 1) and dimensions of $60 \times 60 \text{ km}^2$. The roughness lengths used in this study are displayed in Table 2. Other possibilities to characterise the surface cover include e.g. the enhanced vegetation index (STOY et al., 2013). This index also captures the effects of seasonality in vegetation structure (e.g. agriculture or forest) and they could be accounted for in the estimation of $z_{0,\text{eff}}$. Again, for simplicity reasons this is not done here.

The influence of the surface ruggedness on the drag is difficult to quantify on the scale of the footprint of a wind turbine. Tables which directly specify roughness length for different terrain shapes as in the case of surface cover (e.g. TROEN and LUNDTANG PETERSEN, 1989; WIERINGA, 1992) are not available and existing classifications are very coarse. In meso-scale modelling the effects of sub-grid orography are sometimes parametrised using the standard deviation of the elevation σ_s (e.g. DOMS et al., 2011). However, this measure is sometimes misleading, as e.g. constantly sloping terrain has a high σ_s but exhibits very little ruggedness.

In this study, an index based on the steepness of the slopes is used to define the ruggedness (r_s) within the footprint. The index is based on the concept of the ruggedness index (RIX) which is often used in wind resource assessment applications to classify sites according to their ruggedness and to estimate errors in modelled wind speeds (BOWEN and MORTENSEN, 1996; MORTENSEN and PETERSEN, 1997). The basic idea of this index is to identify slopes upstream of the wind measurement or turbine which exceed a critical value (Θ_{crit}). r_s is then defined as:

$$r_s = \frac{A_{r_s}}{A_{80}}, \quad (2.3)$$

where A_{r_s} is the area inside the 80%-effect level of the footprint exceeding the critical slope and A_{80} is the total area of the 80%-effect level of the footprint. As for the RIX index, the critical slope is defined as $\Theta_{\text{crit}} = 0.3$ in

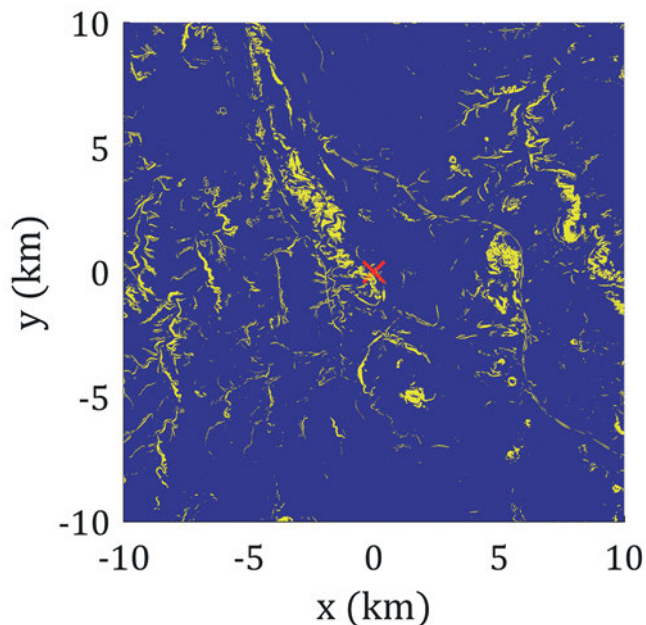


Figure 3: Ruggedness around the mast at Rödeser Berg. Yellow indicates areas exceeding the critical slope $\Theta_{\text{crit}} = 0.3$. The coordinate system is centered at the mast location denoted by the red cross.

this study. This roughly corresponds to the onset of flow separation (WOOD, 1995).

While the RIX-Index only considers the slope of the terrain in the direction of the flow, here, the slope of the terrain is calculated for all directions within a semicircle (0 to 180°) in 1° -steps by shifting the terrain elevation map by 10 m in the respective direction. Linear interpolation is applied to derive the shifted map. Pixels which exceed the critical slope are flagged as ‘rugged’. Using this procedure a ruggedness map of the terrain surrounding the measurement site is created (Figure 3). For each sector r_s is then calculated as the percentage of pixels which are flagged as ‘rugged’ within the 80%-effect area of the footprint climatology. A digital elevation model with a 10 m resolution (Geodäsie, 2015) is used in this analysis.

The procedure described above differs from the RIX defined by BOWEN and MORTENSEN (1996) and MORTENSEN and PETERSEN (1997) in two main points. Firstly, the distance within which the index for the ruggedness is calculated dynamically varies with the extend of the footprint. Secondly, the ruggedness is defined by slopes in all directions rather than just the flow direction and positive and negative slopes both add to the ruggedness rather than cancelling out.

3 Results and discussion

3.1 Turbulence statistics at Rödeser Berg

To investigate the directional behaviour of the turbulence quantities at the measurement site the data was binned in 10° -sectors and the average values were calculated. Since the analysis in this paper is mainly

motivated by wind energy applications, periods with $U_{120} < 4 \text{ m s}^{-1}$ were excluded from the directional analysis. The significance of smaller wind speeds for wind energy applications – e.g. for the loads exerted on the turbine – is expected to be small and the threshold is typical for investigations in the wind energy community. The cup anemometer at 120 m was chosen as it is close to the hub height of a modern wind turbine and was available during the entire measurement period (unlike the sonic anemometers which suffered multiple failures).

Figure 4 displays the directional dependence of turbulence statistics as measured by the sonic anemometers at the different heights for locally neutral conditions ($|L| > 500 \text{ m}$; where L is the Obukhov length). Also, local normalisation (i.e. with u_* at the individual heights) is used in Figure 4. The approach of using local scaling is motivated by the fact that we expect the characteristics of the footprint for the different heights to differ significantly. Later a common height for the normalisation is used to compare the turbulence statistics among different heights (Sections 3.2 and 3.3).

A clear directional pattern is visible for all heights (Figure 4) for the turbulence intensity of the stream-wise component of the wind vector $I_u = \sigma_u / \bar{u}$. For all heights a peak in I_u can be observed at roughly 300 to 320° . Within this direction the upstream area is characterised by the forested ridge extending for approx. 5.8 km (Figure 1). This terrain exhibits high roughness as well as high ruggedness. I_u for wind directions between approx. 350 and 60° is relatively low. Here, the terrain is more open and shows less variations in elevation. Between 180 and 300° the two elevated sonic anemometers (135 and 188 m) show a very similar pattern with a constantly increasing I_u . The measurement at 80 m shows a decline between 180 and 210° . Also, I_u at 80 m is significantly higher than at the top two levels for 180 – 360° . In this sector the vicinity of the mast is forested and orographically complex, while the wider surroundings are more open. Values are similar at all levels between 0 – 90° . Here, open agricultural areas are located much closer to the mast and forested hills are located in a distance of several km. A similar pattern as for I_u can be observed for the surface drag ($u_* u_*^{-1}$), although the variation between the top two measurement heights (135 m and 188 m) appears somewhat smaller.

The integral turbulence statistics for the u component ($\sigma_u u_*^{-1}$) vary between 1.67 and 2.18 for the measurements at 135 m and 188 m, and between 1.90 and 2.26 at 80 m. This is lower than the value that is often given for neutral conditions in flat and homogeneous terrain $\sigma_u u_*^{-1} = 2.4$ (e.g. PANOFSKY and DUTTON, 1984) but slightly higher than roughness sub-layer flows above canopies given by RAUPACH et al. (1996) (1.7) and the values reported by ARNQVIST et al. (2015) (approx. 1.7–1.9) for neutral conditions at a tall profile with a long and homogeneous forest fetch for most sectors. For a site with complex orography FRAGOULIS (1997)

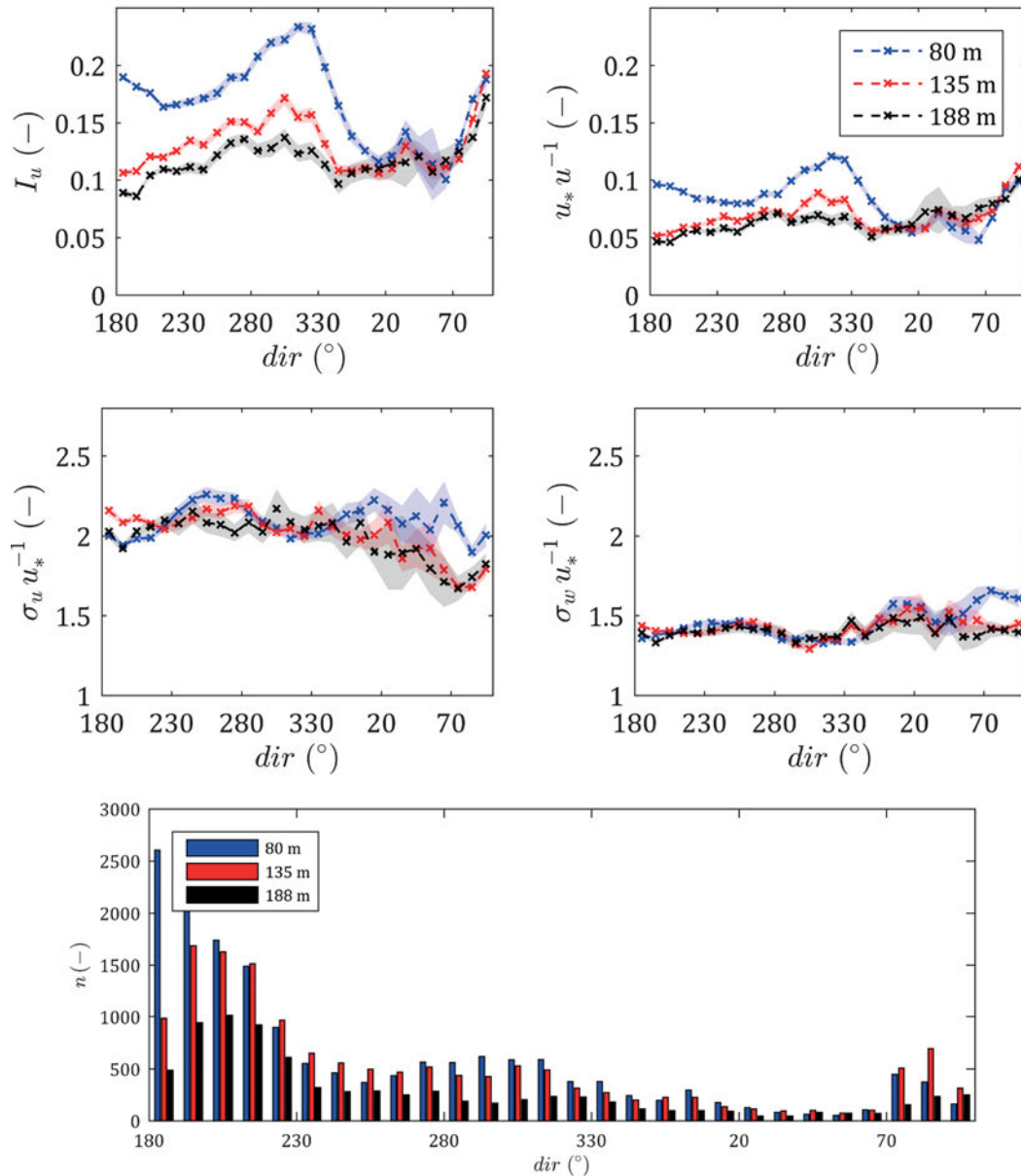


Figure 4: Directional variation of mean turbulence statistics calculated from 10° bins for neutral conditions ($|L| > 500$ m); **top left:** I_u , **top right:** $u_* u_*^{-1}$, **middle left:** $\sigma_u u_*^{-1}$, **middle right:** $\sigma_w u_*^{-1}$, **bottom:** data availability (n); L was determined locally from the individual sonic anemometer; only periods when $U_{120} > 4$ m s $^{-1}$ are included in the analysis; the shaded areas indicate the 95%-confidence intervals derived using Student's t-statistics.

reported values of 2.1–2.4. The directional variation especially at 80 m is to some degree anti-cyclic to the variations in drag and I_u .

$\sigma_w u_*^{-1}$ is in general slightly higher than 1.25 usually assumed over homogeneous terrain. Values range from 1.33 to 1.66 for 80 m and from 1.29 to 1.55 for the upper two heights. Increased values for $\sigma_w u_*^{-1}$ have also been observed at other sites with complex orography (e.g. FRAGOULIS, 1997). $\sigma_w u_*^{-1}$ also shows a similar anti-cyclic pattern for 80 m as $\sigma_u u_*^{-1}$ between 180° and 360°. For the 0–100°-sector $\sigma_w u_*^{-1}$ exhibits relatively strong variations for 80 m and is larger than the observed values for 135 and 188 m. Interestingly, this is also the case

for $\sigma_u u_*^{-1}$. As a note of caution it should be said here that especially for 80 m the data availability is quite low for some of the bins in this sector (the minimum is $n = 25$).

At this point it should be reiterated, that the turbulence statistics were calculated using averaging intervals of 10 minutes, because this is common practice in wind energy applications – e.g. FRAGOULIS (1997) also used 10-minute intervals. Many other micrometeorological studies (including ARNQVIST et al., 2015) use averaging intervals of 30 minutes (e.g. AUBINET et al., 2012). Depending on the integral scales of the different turbulent quantities the choice of the averaging interval will lead to differences in the observed turbulence

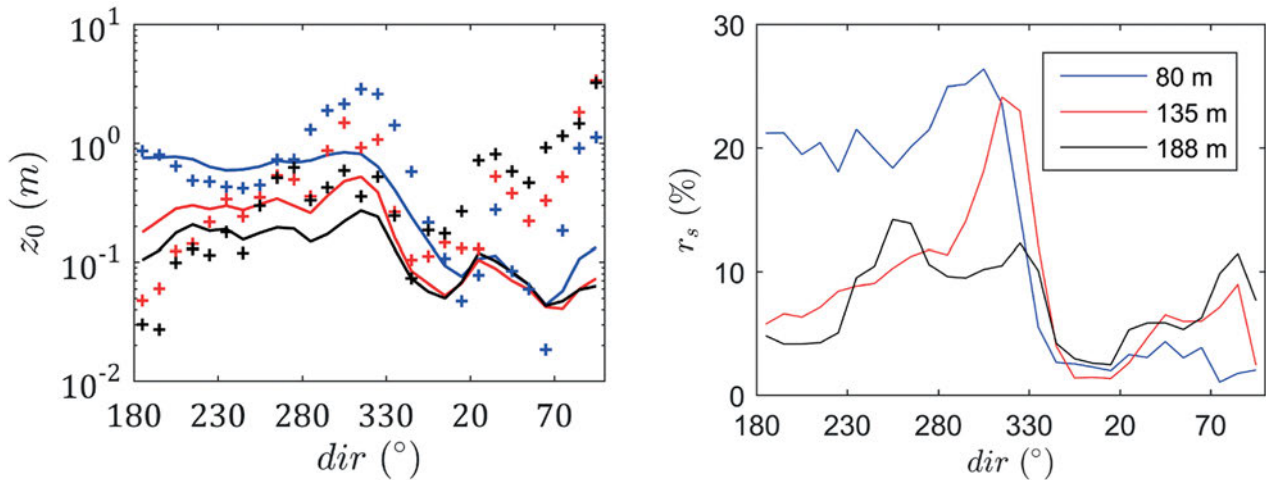


Figure 5: Directional variation of **left:** lines $z_{0,\text{eff}}$ calculated from the footprint climatology (see text) of the 10° bins for neutral conditions ($|L| > 500$ m); the crosses are $z_{0,m}$ calculated from Equation (3.1); **right:** r_s ; note that the left scale is logarithmic, while the right is linear.

statistics (for a detailed discussion see LENSCHOW et al., 1994). We therefore also derived the turbulence characteristics based on 30-minute intervals. If the mean turbulence statistics are compared over all valid sectors, there is very little difference (approx. -1 to 3%) for $\sigma_w u_*^{-1}$ and $u_* u_*^{-1}$. I_u and $\sigma_u u_*^{-1}$ are increased by approx 7 to 13% for the 30-minute intervals with increasing gain for increasing height. Some of the deviation from the typically reported values for $\sigma_u u_*^{-1}$ are, thus, likely to be caused by the 10-minute averaging interval used in this study. This might to some extent be related to the larger turbulent length scales of u . However, also the increasing contribution of meso-scale variations might become visible. At elevated heights the micro-scale turbulence and the meso-scale variations tend to blend into one another and the spectral gap separating the two can disappear (LARSÉN et al., 2016). As for wind turbine loads only the micro-scale turbulence is considered (and important), the choice of a 10-minute averaging interval is more appropriate here.

3.2 The relation between surface characteristics within the footprint and the observed turbulence statistics

The results for the surface characteristics ($z_{0,\text{eff}}$ and r_s) derived from the footprint analysis are displayed in Figure 5. For comparison, also a roughness length which corresponds to the measured turbulence statistics ($z_{0,m}$) is derived using the log-law relationship:

$$z_{0,m} = \exp(\ln(z - d) - \kappa u u_*^{-1}), \quad (3.1)$$

where κ is the von Kármán constant and d is the displacement height. d was estimated from the tree height and density in the direct vicinity of the met mast. It varies by direction with a maximum value of 25 m (for southerly directions with tall and densely spaced trees) and a minimum value of 5 m (for the direction of the

clearing). Due to the high measurement heights the sensitivity to the value of d is rather small. As only neutral conditions are analysed, no stability correction of Equation 3.1 is necessary.

At this point it should be noted that the values of $z_{0,m}$, which are displayed in Figure 5 are intended to facilitate a direct comparison to $z_{0,\text{eff}}$ derived from the surface characteristics of the footprint area. $z_{0,m}$ is also influenced by orography related effects such as e.g. local speed-up effects and should not directly be interpreted as a roughness length. Despite this restriction, $z_{0,m}$ and $z_{0,\text{eff}}$ show similarity in their pattern and magnitudes for all heights between 180° and 360° . However, between 0° and 100° the correlation gets worse and especially for 135 and 188 m, $z_{0,m}$ is significantly higher than $z_{0,\text{eff}}$.

The directional variation of r_s is somewhat similar to $z_{0,\text{eff}}$ with relatively low values for wind directions between 0 and 100° .

Figure 6 displays scatter plots of the relation between different turbulence statistics and surface characteristics. In contrast to Figure 4, turbulence quantities are normalised using the wind speed at a common height (191 m) in Figure 6. A direct comparison of the turbulence statistics across different heights might be misleading as in neutral conditions we expect the wind speed to generally increase with increasing height. On the other hand, the highest values for r_s and $z_{0,\text{eff}}$ are observed at the lowest heights. This fact might introduce some artificial correlation if local scaling is used. The height of 191 m is chosen as it is far away from the surface and thus expected to be less affected by surface effects than lower measurements. It should be noted, however, that the wind speed at 191 m is still influenced by the surface and will, thus, introduce some de-correlation for the turbulence statistics at 135 m and especially at 80 m.

A trend of increasing values of $\sigma_U U_{191}^{-1}$ with increasing r_s and $\ln(z_{0,\text{eff}})$ can be observed for all heights and most values cluster around a more or less linear rela-

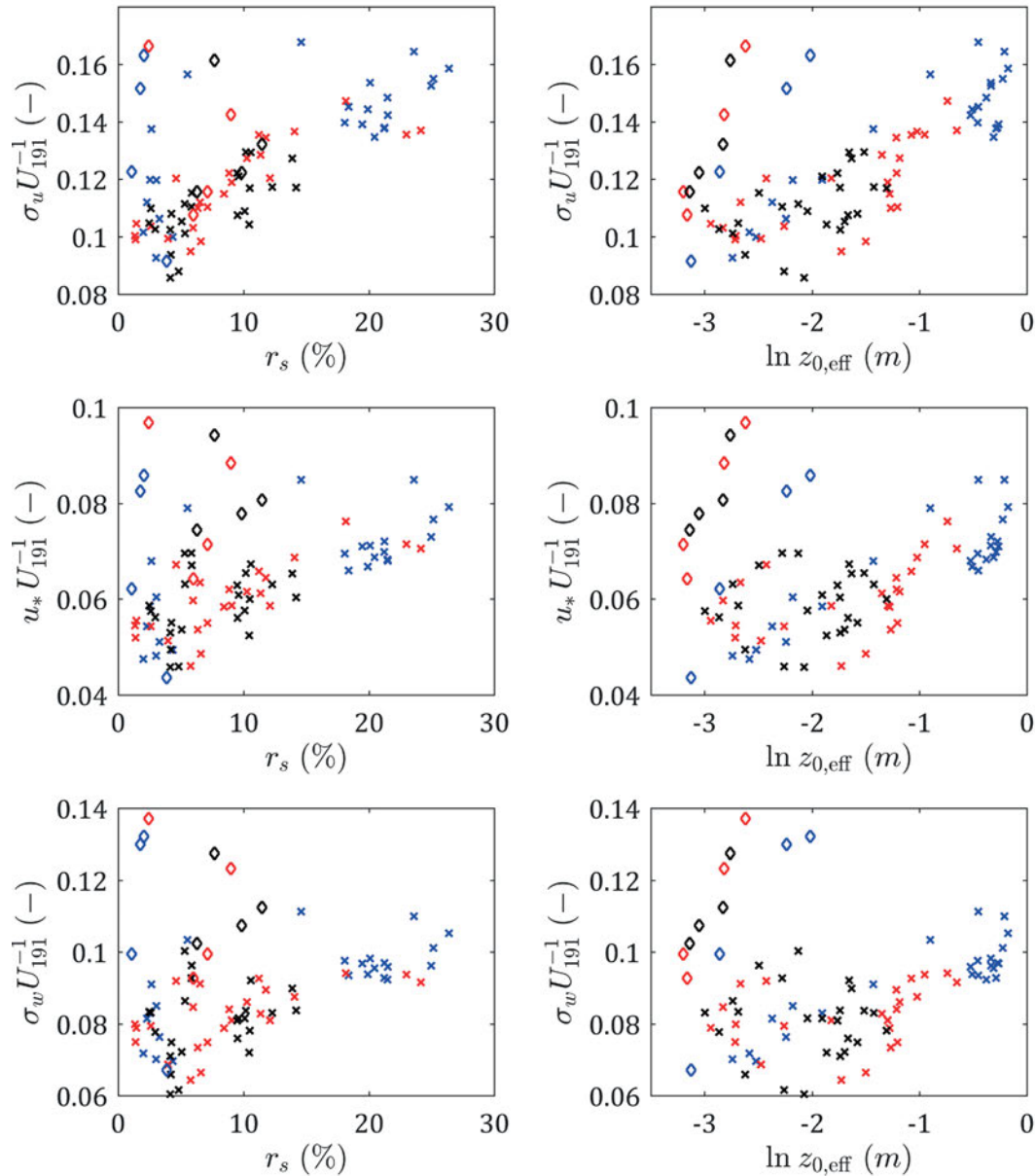


Figure 6: Scatter plots of different turbulence statistics in relation to surface properties within the simulated footprint climatologies; **left column:** normalised turbulence quantities vs the index for ruggedness r_s within the footprint; **right column:** normalised turbulence quantities vs the effective roughness $z_{0,\text{eff}}$ within the footprint; **top:** $\sigma_U U_{191}^{-1}$ **middle:** $u_* U_{191}^{-1}$ and **bottom:** $\sigma_w U_{191}^{-1}$; only periods with neutral conditions ($|L| > 500$ m) have been used; calculations are based on 10° -bins; diamonds indicate bins which lie within $60\text{--}100^\circ$; periods when $U_{120} > 4$ m s $^{-1}$ are excluded from the analysis; for colour coding see Figure 4.

tionship. Several outliers can be observed, which exhibit high values for $\sigma_U U_{191}^{-1}$ but low r_s and $\ln(z_{0,\text{eff}})$. The outliers for 135 and 188 m are associated with the $60\text{--}100^\circ$ -bin where a sharp increase in $\sigma_U U_{191}^{-1}$ but only a moderate increase in r_s can be observed (diamonds in Figure 6). For 80 m another group of outliers can be observed for wind directions between $310\text{--}340^\circ$ where r_s for 80 m starts to drop off but the turbulence intensity remains at a high level (compare also Figure 4). For $\ln(z_{0,\text{eff}})$ no outliers are visible within this sector. However, the scatter for low $\ln(z_{0,\text{eff}})$ is generally slightly higher. The correlation between $\sigma_U U_{191}^{-1}$ and r_s and $\ln(z_{0,\text{eff}})$ is similar (Pearson's r is 0.62 for r_s and 0.60 for $\ln(z_{0,\text{eff}})$).

The correlation for $u_* U_{191}^{-1}$ is weaker than for $\sigma_U U_{191}^{-1}$ and the scatter increases. r is 0.43 and 0.26 for r_s and $\ln(z_{0,\text{eff}})$, respectively. The weakest correlation is observed for $\sigma_w U_{191}^{-1}$ (r is 0.28 and 0.12). The distribution of the points in the scatter plot also suggests that the relationship between r_s and $\sigma_w U_{191}^{-1}$ and $u_* U_{191}^{-1}$ is somewhat stronger than for $\ln(z_{0,\text{eff}})$ when the outliers are excluded.

It is difficult to draw conclusions concerning the relative importance of the terrain ruggedness vs the forest cover within the footprint for the observed turbulence levels, as r_s and $z_{0,\text{eff}}$ are highly correlated in the area around Rödese Berg. Both properties show a high correlation with especially $\sigma_U U_{191}^{-1}$. Nevertheless, some

interesting patterns can be observed when the two are compared.

The ‘outliers’ in the $\sigma_U U_{191}^{-1}$ vs r_s relationship are directed towards a turbulence level but low r_s . Points with high r_s and low $\sigma_U U_{191}^{-1}$ are not observed. This is also true to some extent for the $\sigma_w U_{191}^{-1}$ and $u_* U^{-1}$. This suggests that the ruggedness is an important factor in turbulence production but r_s does not capture all effects responsible for turbulence production. For $\ln(z_{0,\text{eff}})$ the outliers are also directed towards high turbulence and low $\ln(z_{0,\text{eff}})$, however, the lower boundary is less clear.

Much of the increased scatter which is found in the relationship between the turbulence quantities and r_s and $\ln(z_{0,\text{eff}})$, respectively, is related to wind sectors between 60–100°. It is interesting to note that within this sector also the turbulence statistics show some differences when compared to the other wind directions. $\sigma_u u_*^{-1}$ is reduced for the 135 and 188 m measurements and $\sigma_w u_*^{-1}$ is increased for 80 m. For these directions the Schreckenbergl and the Gudenberg start to move into the footprint of the measurements at Rödeser Berg (Figure 1). With a maximum elevation of 568 m it is significantly higher than Rödeser Berg. The presence of this relatively large orographical obstacle is probably not well represented in the definition of r_s , as it only accounts for the slope and not the height of the ruggedness elements.

Summarising the observations, especially r_s inside the footprint area seems to be a promising way to explain the directional variations in $\sigma_u U_{191}^{-1}$ induced by the orography. It should, however, be noted that r_s is only an approximation for the surface ruggedness. The results will depend to some degree on the choice of Θ_{crit} , which here is motivated by the onset of flow separation. The critical slope for flow separation will vary with surface cover i.e. be smaller for forested hills than for bare soil (FINNIGAN and BELCHER, 2004).

Also due to the categorical nature of r_s the calculation of a footprint-weighted ruggedness is not as straightforward as for $z_{0,\text{eff}}$ and is not attempted here. Nevertheless, it is intuitive that the effect of orographic features will vary according to their location within the footprint area.

3.3 Turbulence intensity in comparison to existing design guidelines and the influence of atmospheric stability

Turbulence intensity of the horizontal wind speed is one of the key parameters used in the site suitability analysis for wind turbines (IEC, 2005a). To model the expected loads during the life time of a wind turbine the turbulence intensity as a function of wind speed is required. This section therefore focuses on the analysis of this quantity.

In standard load modelling applications the representative turbulence intensity $I_{\text{rep}} = \sigma_{\text{rep}}/U$ is often described by the ‘normal turbulence model’ (NTM)

according to IEC (2005a):

$$\sigma_{\text{rep}} = I_{\text{ref}}(0.75U + 5.6 \text{ m s}^{-1}), \quad (3.2)$$

where I_{ref} is a dimensionless constant which depends on the turbine class (for the different turbine classes see also Figure 7). In site assessment applications I_{rep} is compared to the 90 %-percentile of the measured turbulence intensity of the horizontal wind speed to see if a turbine is suitable for a specific site. From measurements this is usually approximated as $I_{U90} = I_U + 1.28\sigma_{I_U}$, where I_U is the mean turbulence intensity and σ_{I_U} is the standard deviation of the turbulence intensity. Stability effects are not parametrised in this formulation. For the analysis in this paper I_{U90} and I_U are calculated using wind-speed bins with a width of 1 m s^{-1} .

As shown in Section 3.2 turbulence statistics strongly vary with wind direction. To allow for the exploration of other effects on the turbulence intensity the analysis in this section is therefore confined to a narrow sector including the main wind direction (180–220°).

Also, unlike in the previous sections cup anemometers are used to derive the turbulence intensity. This is mainly motivated by two facts. Firstly, as mentioned in Section 2.2, there were multiple instrument failures on the sonic anemometers. The set of concurrent measurements over the wide height range is rather limited for the sonics. Using cup anemometers the data base for the analysis in this section is significantly enhanced. Secondly, it is common practice in the wind energy community to use cup rather than sonic to measure turbulence intensity. It should be noted again that the standard deviation of the horizontal wind speed between a sonic and a cup measurement is expected to differ. As the sonic is able to resolve smaller turbulent scales, it will usually measure slightly higher turbulence intensities.

Figure 7 displays the standard deviation of the wind speed measured by cup anemometers (σ_U) at 60, 120 and 191 m height normalised by the wind speed at 120 m (U_{120}) as a function of U_{120} . The heights roughly reflect the lower tip, hub and upper tip heights of a modern wind turbine. The somewhat unusual normalisation is motivated by a better direct comparability of the variance within the wind field at the different heights. In load simulations it is common practice to specify a target variance of the wind field and keep this constant across the whole modelling domain. This stems from classical surface layer theory in homogeneous terrain, which is, however, questionable for heterogeneous surfaces like in the current setup.

The first striking observation is that there is a relatively strong variation of the turbulence levels at the different heights with strongly decreasing turbulence with height. Especially the difference between the 60 m and 120 m measurements is large and in the order or even exceeding the differences between the different standard turbulence classes for wind turbine design (Figure 7). The behaviour of σ_U with height from other experiments is not entirely clear. While GARRATT (1994) suggests an

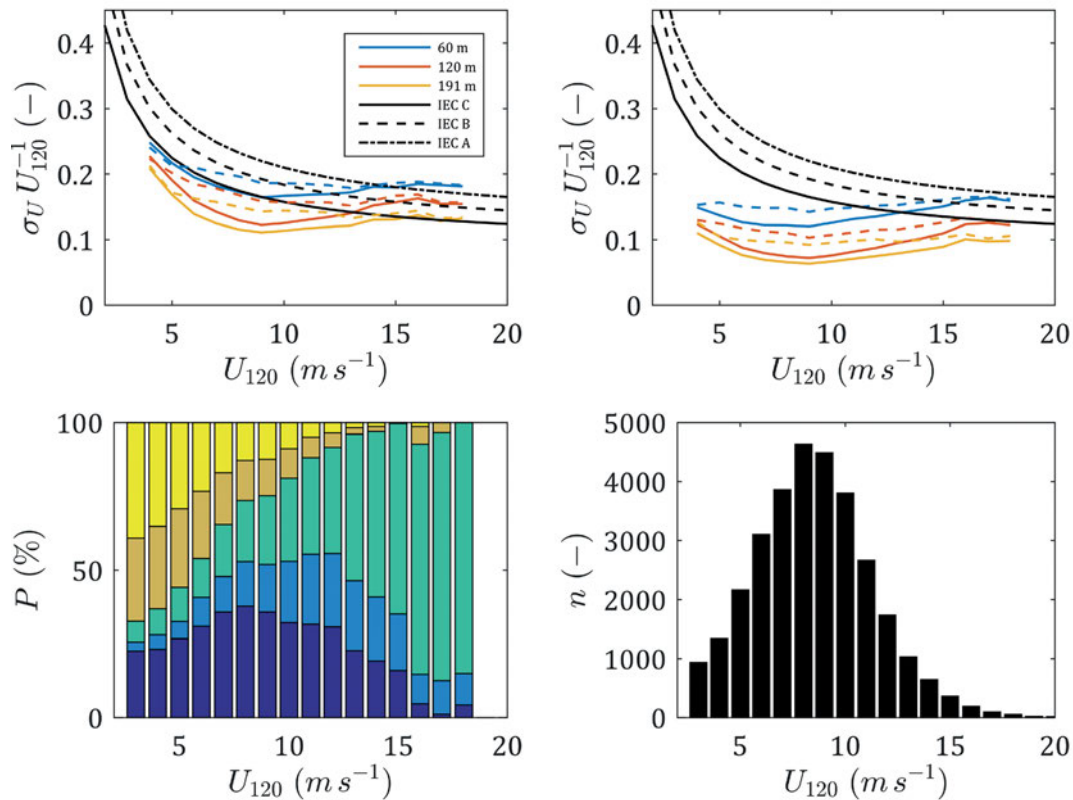


Figure 7: **Top left:** σ_U/U_{120} by wind speed for 180–220°; the solid lines indicate I_{U90} as defined by equation 3.2 for all measurements, dashed lines are only neutral conditions ($|L| > 500$ m); the black lines show the normal turbulence model; turbulence class A ($I_{ref} = 0.16$); turbulence class B ($I_{ref} = 0.14$); turbulence class C ($I_{ref} = 0.12$); **top right:** same as the left panel but the bin-wise mean (rather than the 90-%-percentile) of the observed turbulence intensities is displayed. **bottom left:** occurrence of atmospheric stability classes for different wind speeds as observed at 135 m; dark blue denotes stable ($0 \text{ m} < L < 200 \text{ m}$), light blue slightly stable ($200 \text{ m} < L < 500 \text{ m}$), green neutral ($|L| > 500 \text{ m}$), orange slightly unstable ($-200 \text{ m} > L > -500 \text{ m}$) and yellow unstable ($0 \text{ m} > L > -200 \text{ m}$) conditions; **bottom right:** data availability for the different wind-speed bins; only bins with more than 20 observations are included.

almost constant σ_U throughout most of the atmospheric boundary layer, ARYA (2001) suggest an exponential reduction which is equal to the reduction in σ_w . Profiles reported in a high roughness environment over a homogeneous forest in Sweden (ARNQVIST et al., 2015) indicate a reduction of σ_U between comparable heights (60 and 135 m) which is smaller than the reduction in Figure 7. As demonstrated in Section 3.2, one of the main reasons for this observation is the variation of the surface characteristics within the footprint of the different measurement heights (Figure 5).

As the IEC standard (IEC, 2005a) only defines three different turbulence classes, it is unlikely that the absolute turbulence levels will match one of the defined classes. It is thus more interesting to compare the shape of the observed to the empirically derived curve in IEC (2005a). A prominent feature of I_U as well as I_{U90} is that they show a minimum between approx. 8–10 m s^{-1} (Figure 7). For higher wind speeds the turbulence intensities are increasing again. This behaviour is contrary to the shape of the NTM, which is monotonically decreasing. The pattern of the observed atmospheric stability at 135 m shows an interesting correlation with the mean turbulence intensity and I_{U90} . At low wind

speeds, where turbulence intensities are high, unstable conditions are dominant. With increasing wind speed the percentage of stable conditions increases and reaches a maximum at about the same wind speeds as where the minimum of the turbulence intensities is observed. For the classification according to the observed Obukhov length see caption of Figure 7.

If only neutral conditions are considered, no clear minimum is visible for neither I_{U90} nor I_U . In fact, within the wind speed range where the maximum number of stable conditions is found, also the maximum difference between the overall and neutral statistics can be observed. For wind energy applications this observation is highly relevant, as the wind speed range between 6–12 m s^{-1} is very important for fatigue loads on onshore turbines.

There are different possible mechanisms which might be responsible for the observation of this correlation between atmospheric stability and wind speed. The first is that the influence of the stable stratification dampens the frictional forces which can lead to an increased flow at higher levels and the formation of a low level jet (LLJ). The LLJ is usually defined by a wind speed maximum in the first few hundred meters above ground.

It has been studied over several decades (BLACKADAR, 1957; STENSRUD, 1996). More recently, its importance for resource estimation in wind energy applications in northern Germany has been suggested (EMEIS, 2014; LAMPERT et al., 2016). Also in forested low mountain ranges in Germany the frequent occurrence of LLJs has been reported (SERAFIMOVICH et al., 2017).

An often used definition of the LLJ is a wind maximum which is at least 2 m s^{-1} higher than the minimum aloft (STULL, 1988). However, only very few profiles fulfill this criterion within the first 200 m above ground at Rödeser Berg. Although there are more profiles where the wind speed is decreasing with height at the top measurement height(s), a clear identification of LLJ-events with the mast data is difficult. In fact, the reported typical heights of LLJ reported from other sites vary from between 100–200 m (e.g. BANTA et al., 2002; BAAS et al., 2009) up to several hundred meters (e.g. BONNER, 1968; ZHANG et al., 2006). EMEIS (2014) found that the persistence of a LLJ is limited by a critical shear below the jet, which is dependent of the Richardson number (EMEIS, 2017). This can also set a lower limit to the height of the jet core. The typical height of the LLJs at Rödeser Berg might thus be too high to be reliably detected by the mast measurement.

The second possible reason for increased wind speeds in stable conditions at Rödeser Berg is the interaction between stability and orographic effects. The speed-up over hills and ridges can be significantly increased in stable conditions (e.g. CARRUTHERS and CHOUARTON, 1982; BRADLEY, 1983; COPPIN et al., 1994). Moreover, if the boundary layer is very shallow, the flow might be forced around the hill in diverging flow lines (SNYDER et al., 1985). In a shallow boundary layer the mast measurements might even be above the turbulent boundary layer. A more detailed investigation of the flow over the hill and speed-up effects is currently done using a spatial network of profiling and scanning lidars in the framework of the New European Wind Atlas Project (MANN et al., 2017).

There are only few studies reporting explicitly on the distribution of atmospheric stability and σ_U as a function of wind speed. SATHE et al. (2013) investigated the influence of atmospheric stability on wind turbine loads. Their analysis also showed a clear reduction of σ_U with increasing stability (they used the Obukhov length) for a homogeneous site. The stability conditions over several different coastal sites generally indicated a decreasing occurrence of stable conditions with increasing wind speed. However, the stability distributions were derived from either eddy co-variance measurements close to the ground or profile measurements.

For a mildly complex site in the western USA WHARTON and LUNDQUIST (2012) reported similar observations as found at Rödeser Berg. The lowest wind speeds and highest turbulence intensities were found in unstable conditions. Their observations even indicated the highest wind speeds for stable conditions at their site. At Rödeser Berg for wind speeds above approx. 12 m s^{-1}

neutral conditions begin to dominate and the mean wind speed during neutral conditions is larger than during stable conditions. This is in line with the fact that for high wind speeds in stable conditions the formation of low level jets is limited to greater heights as mechanical mixing will be induced if the shear exceeds a critical value (EMEIS, 2017) and the stable stratification will not longer persist. Also, the occurrence of the diverging flow lines is dependent on the wind speed and is more likely to be observed in lower wind speed conditions (SNYDER et al., 1985).

4 Conclusion and outlook

Linking surface properties to observed turbulence statistics provides a difficult task in complex and patchy terrain. At Rödeser Berg a directional analysis of turbulence statistics in relation to the surface characteristics within the modelled footprint was carried out. Especially the normalised standard deviation of the wind velocity in the direction of the flow lines ($\sigma_u U_{191}^{-1}$) showed a high correlation with the ruggedness and the effective roughness for all heights and most wind-direction sectors.

These results indicate that, despite the simplicity of the approach, footprint modelling, as frequently used in the flux community, can provide a valuable tool for relating measured turbulence statistics to observations. In wind energy applications footprint modelling can be used to e.g. identifying wind sectors for which high turbulence levels are to be expected. In combination with simple surface metrics its main benefit lies in the simple evaluation and possible classification of wind turbine sites.

The conclusion regarding the effects of terrain ruggedness vs high roughness areas within the footprint on turbulence quantities are less conclusive as ruggedness and roughness are strongly correlated in the area surrounding the measurement site.

Effective roughness length ($z_{0,\text{eff}}$) and the ruggedness index (r_s) as used in this study are simplifications and the limit of the explanatory power for the variation of the turbulence levels was visible in the wind direction sector where a large orographical obstacle is present. Besides experimental campaigns, further validation studies of footprint tools for wind energy applications should include comparison with more complex models such as large eddy simulations. Within the simulation environment the range of the validity of simple analytical footprint approaches can be evaluated by switching certain terrain features in the modelling environment ‘on’ and ‘off’.

The observed behaviour of the turbulence intensity showed significant deviations from the normal turbulence model suggested in IEC (2005a) for the investigated sector. The reason for this is likely to be the distribution of atmospheric stability. The differences between the normalised standard deviation of the horizontal wind speed for all stability conditions and only neutral cases

are significant compared to design guidelines of wind turbines. They exceed the difference between the different turbulence classes specified in the current standard for wind turbine design (IEC, 2005a). From an applied point of view it is interesting to note that this effect occurs within a wind speed range which is highly relevant for the fatigue loads experienced by a wind turbine. Unfortunately, at higher wind speeds this effect vanishes and periods with high wind speeds and high turbulence result. This suggests that in the next generation wind farm design tools and models for estimating the site specific turbulence conditions should include the effect of atmospheric stability in addition to the terrain effects. While some first progress to include atmospheric stability in load simulations (e.g. SATHE et al., 2011; PARK et al., 2014) and wake modelling (e.g. ÖZDEMİR et al., 2013) has been made, the inclusion of atmospheric stability in site assessment still remains a difficult issue.

The strong variation of the standard deviation of the horizontal wind speed (σ_U) with height suggests that the assumption of a turbulence field with a constant variance across the modelling domain might not be adequate for wind turbines with large rotors in heterogeneous terrain.

Acknowledgments

The authors would like to acknowledge the technical support of RICHARD DÖPFER, KLAUS OTTO and ZOUHAIR KHADIRI and many others at IWES during the measurements. We would also like to thank the two anonymous reviewers who greatly helped to improve the quality of this manuscript with their critical comments and suggestions. The work for this publication was funded by the following project: Windenergie im Binnenland II (Förderkennzeichen 0325171A) funded by the German Federal Ministry of Economics.

References

- ALLEN, T., A.R. BROWN, 2002: Large-eddy simulation of turbulent separated flow over rough hills. – *Bound.-Layer Meteor.* **102**, 177–198, DOI: [10.1023/A:1013155712154](https://doi.org/10.1023/A:1013155712154).
- ARNQVIST, J., A. SEGALINI, E. DELLWIK, H. BERGSTRÖM, 2015: Wind statistics from a forested landscape. – *Bound.-Layer Meteor.* **156**, 53–71, DOI: [10.1007/s10546-015-0016-x](https://doi.org/10.1007/s10546-015-0016-x).
- ARYA, S.P., 2001: Introduction to micrometeorology. – International geophysics series **79**, – Academic Press, San Diego, California and London.
- AUBINET, M., T. VESALA, D. PAPALE (Eds.), 2012: Eddy Covariance. – Springer, Dordrecht.
- BAAS, P., F.C. BOSVELD, H. KLEIN BALTINK, A.A.M. HOLTSLAG, 2009: A climatology of nocturnal low-level jets at cabauw. – *J. Appl. Meteor. Climatol.* **48**, 1627–1642, DOI: [10.1175/2009JAMC1965.1](https://doi.org/10.1175/2009JAMC1965.1).
- BALDOCCHI, D., 2014: Measuring fluxes of trace gases and energy between ecosystems and the atmosphere – the state and future of the eddy covariance method. – *Global Change Biology* **20**, 3600–3609, DOI: [10.1111/gcb.12649](https://doi.org/10.1111/gcb.12649).
- BANTA, R., R.K. NEWSOM, J.K. LUNDQUIST, Y.L. PICHUGINA, R.L. COULTER, L. MAHRT, 2002: Nocturnal low-level jet characteristics over Kansas during CASES-99. – *Bound.-Layer Meteor.* **105**, 221–252, DOI: [10.1023/A:1019992330866](https://doi.org/10.1023/A:1019992330866).
- BERKHOUT, V., S. FAULSTICH, B. HAHN, J. HIRSCH, K. LINKE, M. NEUSCHÄFER, S. PFAFFEL, K. RAFIK, K. ROHRIG, SACK, ANDRE, STARK, ELISABETH, L. SCHULDT, M. ZIESSE, 2015: Wind energy report Germany 2014. – http://windmonitor.iwes.fraunhofer.de/opencms/export/sites/windmonitor/img/Windenergie_Report_2014.pdf.
- BLACKADAR, A.K., 1957: Boundary layer wind maxima and their significance for the growth of nocturnal inversions. – *Bull. Amer. Meteor. Soc.* **38**, 283–290.
- BONNER, W.D., 1968: Climatology of the low level jet. – *Mon. Wea. Rev.* **96**, 833–850, DOI: [10.1175/1520-0493\(1968\)096<0833:COTLLJ>2.0.CO;2](https://doi.org/10.1175/1520-0493(1968)096<0833:COTLLJ>2.0.CO;2).
- BOUDREAU, L.E., 2015: Reynolds-averaged Navier-Stokes and large-eddy simulation over and inside inhomogeneous forests. – Ph.D. thesis, DTU Wind Energy, Denmark, DTU Wind Energy PhD-0042.
- BOWEN, A.J., N.G. MORTENSEN, 1996: Exploring the limits of wasp the wind atlas analysis and application program. – In: European Wind Energy Conference and Exhibition 1996, 584–587.
- BRADLEY, E.F., 1980: An experimental study of the profiles of wind speed, shearing stress and turbulence at the crest of a large hill. – *Quart. J. Roy. Meteor. Soc.* **106**, 101–123, DOI: [10.1002/qj.49710644708](https://doi.org/10.1002/qj.49710644708).
- BRADLEY, E., 1983: The influence of thermal stability and angle of incidence on the acceleration of wind up a slope. – *J. Wind Engin. Industrial Aerodyn.* **15**, 231–242, DOI: [10.1016/0167-6105\(83\)90193-9](https://doi.org/10.1016/0167-6105(83)90193-9).
- BROWN, A.R., J.M. HOBSON, N. WOOD, 2001: Large-eddy simulation of neutral turbulent flow over rough sinusoidal ridges. – *Bound.-Layer Meteor.* **98**, 411–441, DOI: [10.1023/A:1018703209408](https://doi.org/10.1023/A:1018703209408).
- BUNDESAMT FÜR KARTOGRAPHIE UND GEODÄSIE, 2015: Digitales Geländemodell Gitterweite 10 m DGM10. – <http://www.geodatenzentrum.de/docpdf/dgm10.pdf> (accessed at 03.08.2016).
- CALLIES, D., 2015: Analyse des Potenzials der Onshore-Windenergie in Deutschland unter Berücksichtigung von technischen und planerischen Randbedingungen. – Ph.D. thesis, Universität Kassel, Hessen.
- CARRUTHERS, D.J., T.W. CHOULARTON, 1982: Airflow over hills of moderate slope. – *Quart. J. Roy. Meteor. Soc.* **108**, 603–624, DOI: [10.1002/qj.49710845708](https://doi.org/10.1002/qj.49710845708).
- CHOUGULE, A., J. MANN, A. SEGALINI, E. DELLWIK, 2015: Spectral tensor parameters for wind turbine load modeling from forested and agricultural landscapes. – *Wind Energy* **18**, 469–481, DOI: [10.1002/we.1709](https://doi.org/10.1002/we.1709).
- COPPIN, P.A., E.F. BRADLEY, J.J. FINNIGAN, 1994: Measurements of flow over an elongated ridge and its thermal stability dependence: The mean field. – *Bound.-Layer Meteor.* **69**, 173–199, DOI: [10.1007/BF00713302](https://doi.org/10.1007/BF00713302).
- DOMS, G., J. FÖRSTNER, E. HEISE, H.J. HERZOG, M.R. MIRONOV, 2011: A description of the nonhydrostatic regional COSMO model: Part II: Physical Parameterization. – Deutscher Wetterdienst, Offenbach, Germany.
- EMEIS, S., 2014: Wind speed and shear associated with low-level jets over Northern Germany. – *Meteorol. Z.* **23**, 295–304, DOI: [10.1127/0941-2948/2014/0551](https://doi.org/10.1127/0941-2948/2014/0551).
- EMEIS, S., 2017: Upper limit for wind shear in stably stratified conditions expressed in terms of a bulk richardson number. – *Meteorol. Z.*, published online, DOI: [10.1127/metz/2017/0828](https://doi.org/10.1127/metz/2017/0828).
- FINNIGAN, J.J., S.E. BELCHER, 2004: Flow over a hill covered with a plant canopy. – *Quart. J. Roy. Meteor. Soc.* **130**, 1–29, DOI: [10.1256/qj.02.177](https://doi.org/10.1256/qj.02.177).

- FOKEN, T., 2013: Application of footprint models for wind turbine locations. – *Meteorol. Z.* **22**, 111–115, DOI: [10.1127/0941-2948/2012/0390](https://doi.org/10.1127/0941-2948/2012/0390).
- FOKEN, T., 2017: *Micrometeorology*. – Springer, ebook.
- FOKEN, T., M.Y. LECLERC, 2004: Methods and limitations in validation of footprint models. – *Agricult. Forest Meteor.* **127**, 223–234, DOI: [10.1016/j.agrformet.2004.07.015](https://doi.org/10.1016/j.agrformet.2004.07.015).
- FRAGOULIS, A., 1997: The complex terrain wind environment and its effects on the power output and loading of wind turbines. – In: 35th Aerospace Sciences Meeting and Exhibit.
- GARRATT, J.R., 1994: *The atmospheric boundary layer*. – Cambridge atmospheric and space science series, Univ. Press, Cambridge.
- GÖCKEDE, M., C. REBMANN, T. FOKEN, 2004: A combination of quality assessment tools for eddy covariance measurements with footprint modelling for the characterisation of complex sites. – *Agricult. Forest Meteor.* **127**, 175–188, DOI: [10.1016/j.agrformet.2004.07.012](https://doi.org/10.1016/j.agrformet.2004.07.012).
- GÖCKEDE, M., T. MARKKANEN, C.B. HASAGER, T. FOKEN, 2006: Update of a footprint-based approach for the characterisation of complex measurement sites. – *Bound.-Layer Meteor.* **118**, 635–655, DOI: [10.1007/s10546-005-6435-3](https://doi.org/10.1007/s10546-005-6435-3).
- GRANT, E.R., A.N. ROSS, B.A. GARDINER, S.D. MOBBS, 2015: Field observations of canopy flows over complex terrain. – *Bound.-Layer Meteor.* **156**, 231–251, DOI: [10.1007/s10546-015-0015-y](https://doi.org/10.1007/s10546-015-0015-y).
- HANNA, S.R., J.C. CHANG, 1993: Hybrid plume dispersion model (hpdm) improvements and testing at three field sites. – *Atmos. Env. Part A General Topics* **27**, 1491–1508, DOI: [10.1016/0960-1686\(93\)90135-L](https://doi.org/10.1016/0960-1686(93)90135-L).
- HASAGER, C.B., N.O. JENSEN, 1999: Surface-flux aggregation in heterogeneous terrain. – *Quart. J. Roy. Meteor. Soc.* **125**, 2075–2102, DOI: [10.1002/qj.49712555808](https://doi.org/10.1002/qj.49712555808).
- HASAGER, C.B., N.W. NIELSEN, N.O. JENSEN, E. BOEGH, J.H. CHRISTENSEN, E. DELLWIK, H. SOEGAARD, 2003: Effective roughness calculated from satellite-derived land cover maps and hedge-information used in a weather forecasting model. – *Bound.-Layer Meteor.* **109**, 227–254, DOI: [10.1023/A:1025841424078](https://doi.org/10.1023/A:1025841424078).
- HORST, T., 2000: An intercomparison of measures of special inhomogeneity for surface fluxes of passive scalars. – In: *Proceedings of the 14th Symposium on Boundary Layer and Turbulence*, Aspen, CO. American Meteorological Society, Boston, MA, 11–14.
- IEC, 2005a: IEC 61400-1 wind turbines – part 1: Design requirements. – https://webstore.iec.ch/preview/info_iec61400-1%7Bed3.0%7Den.pdf.
- IEC, 2005b: IEC 61400-12-1 wind turbines – part 12-1: Power performance measurements of electricity producing wind turbines. – https://www.vde-verlag.de/iec-normen/preview-pdf/info_iec61400-12-1%7Bed1.0%7Den.pdf.
- KAIMAL, J.C., J.J. FINNIGAN, 1994: *Atmospheric boundary layer flows: Their structure and measurement*. – Oxford University Press, New York.
- KLAAS, T., L. PAUSCHER, D. CALLIES, 2015: Lidar-mast deviations in complex terrain and their simulation using cfd. – *Meteorol. Z.* **24**, 591–603, DOI: [10.1127/metz/2015/0637](https://doi.org/10.1127/metz/2015/0637).
- KLJUN, N., M.W. ROTACH, H.P. SCHMID, 2002: A three-dimensional backward lagrangian footprint model for a wide range of boundary-layer stratifications. – *Bound.-Layer Meteor.* **103**, 205–226, DOI: [10.1023/A:1014556300021](https://doi.org/10.1023/A:1014556300021).
- KLJUN, N., P. CALANCA, M.W. ROTACH, H.P. SCHMID, 2015: A simple two-dimensional parameterisation for flux footprint prediction (ffp). – *Geosci. Model Develop.* **8**, 3695–3713, DOI: [10.5194/gmd-8-3695-2015](https://doi.org/10.5194/gmd-8-3695-2015).
- LAMPERT, A., B. BERNALTE JIMENEZ, G. GROSS, D. WULFF, T. KENULL, 2016: One-year observations of the wind distribution and low-level jet occurrence at Braunschweig, North German Plain. – *Wind Energy* **19**, 1807–1817, DOI: [10.1002/we.1951](https://doi.org/10.1002/we.1951).
- LARSÉN, X.G., S.E. LARSEN, E.L. PETERSEN, 2016: Full-scale spectrum of boundary-layer winds. – *Bound.-Layer Meteor.* **159**, 349–371, DOI: [10.1007/s10546-016-0129-x](https://doi.org/10.1007/s10546-016-0129-x).
- LECLERC, M.Y., T. FOKEN, 2014: *Footprints in Micrometeorology and Ecology*. – Springer Berlin Heidelberg.
- LENSCHOW, D.H., J. MANN, L. KRISTENSEN, 1994: How long is long enough when measuring fluxes and other turbulence statistics?. – *J. Atmos. Oceanic Technol.* **11**, 661–673, DOI: [10.1175/1520-0426\(1994\)011<0661:HLILEW>2.0.CO;2](https://doi.org/10.1175/1520-0426(1994)011<0661:HLILEW>2.0.CO;2).
- MANN, J., 1994: The spatial structure of neutral atmospheric surface-layer turbulence. – *J. Fluid Mech.* **273**, 141, DOI: [10.1017/S0022112094001886](https://doi.org/10.1017/S0022112094001886).
- MANN, J., N. ANGELOU, J. ARNQVIST, D. CALLIES, E. CANTERO, R.C. ARROYO, M. COURTNEY, J. CUXART, E. DELLWIK, J. GOTTSCHALL, S. IVANELL, P. KÜHN, G. LEA, J.C. MATOS, J.M.L.M. PALMA, L. PAUSCHER, A. PEÑA, J.S. RODRIGO, S. SÖDERBERG, N. VASILJEVIC, C.V. RODRIGUES, 2017: Complex terrain experiments in the new european wind atlas. – *Philosophical Transactions of the Royal Society of London A: Mathematical, Physical and Engineering Sciences* **375**, DOI: [10.1098/rsta.2016.0101](https://doi.org/10.1098/rsta.2016.0101).
- MARKKANEN, T., G. STEINFELD, N. KLJUN, S. RAASCH, T. FOKEN, 2009: Comparison of conventional lagrangian stochastic footprint models against LES driven footprint estimates. – *Atmos. Chem. Phys.* **9**, 5575–5586, DOI: [10.5194/acp-9-5575-2009](https://doi.org/10.5194/acp-9-5575-2009).
- MORTENSEN, N.G., E.L. PETERSEN, 1997: Influence of topographical input data on the accuracy of wind flow modelling in complex terrain. – In: *1997 European Wind Energy Conference*, 317–320.
- NEFF, D.E., R.N. MERONEY, 1998: Wind-tunnel modeling of hill and vegetation influence on wind power availability. – *J. Wind Engin. Industrial Aerodyn.* **74-76**, 335–343, DOI: [10.1016/S0167-6105\(98\)00030-0](https://doi.org/10.1016/S0167-6105(98)00030-0).
- ÖZDEMİR, H., M. VERSTEG, A. BRAND, 2013: Improvements in ecn wake model. – In: *International Conference on Aerodynamics of Offshore Wind Energy Systems and Wakes (ICOWES2013)*, volume 1.
- PANOFSKY, H.A., J.A. DUTTON, 1984: *Atmospheric turbulence: Models and methods for engineering applications*. – Wiley, New York and Chichester.
- PARK, J., S. BASU, L. MANUEL, 2014: Large-eddy simulation of stable boundary layer turbulence and estimation of associated wind turbine loads. – *Wind Energy* **17**, 359–384, DOI: [10.1002/we.1580](https://doi.org/10.1002/we.1580).
- PATTON, E.G., G.G. KATUL, 2009: Turbulent pressure and velocity perturbations induced by gentle hills covered with sparse and dense canopies. – *Bound.-Layer Meteor.* **133**, 189–217, DOI: [10.1007/s10546-009-9427-x](https://doi.org/10.1007/s10546-009-9427-x).
- PAUSCHER, L., N. VASILJEVIC, D. CALLIES, G. LEA, J. MANN, T. KLAAS, J. HIERONIMUS, J. GOTTSCHALL, A. SCHWESIG, M. KÜHN, M. COURTNEY, 2016: An inter-comparison study of multi- and dbs lidar measurements in complex terrain. – *Remote Sens.* **8**, 782, DOI: [10.3390/rs8090782](https://doi.org/10.3390/rs8090782).
- PHILIP, J., 1997: Blending and internal boundary-layer heights, and shear stress. – *Bound.-Layer Meteor.* **84**, 85–98, DOI: [10.1023/A:1000345015838](https://doi.org/10.1023/A:1000345015838).
- POGGI, D., G.G. KATUL, 2007: An experimental investigation of the mean momentum budget inside dense canopies on narrow gentle hilly terrain. – *Agricult. Forest Meteor.* **144**, 1–13, DOI: [10.1016/j.agrformet.2007.01.009](https://doi.org/10.1016/j.agrformet.2007.01.009).
- POGGI, D., G.G. KATUL, 2008: Turbulent intensities and velocity spectra for bare and forested gentle hills: Flume

- experiments. – *Bound.-Layer Meteor.* **129**, 25–46, DOI: [10.1007/s10546-008-9308-8](https://doi.org/10.1007/s10546-008-9308-8).
- RANNIK, Ü., A. SOGACHEV, T. FOKEN, M. GÖCKEDE, N. KLJUN, M.Y. LECLERC, T. VESALA, 2012: Footprint analysis. – In: M. AUBINET, T. VESALA, D. PAPALE (Eds.): *Eddy Covariance*. – Springer Netherlands, Dordrecht, 211–261, DOI: [10.1007/978-94-007-2351-1_8](https://doi.org/10.1007/978-94-007-2351-1_8).
- RAUPACH, M., J. FINNIGAN, Y. BRUNEL, 1996: Coherent eddies and turbulence in vegetation canopies: The mixing-layer analogy. – *Bound.-Layer Meteor.* **78**, 351–382, DOI: [10.1007/BF00120941](https://doi.org/10.1007/BF00120941).
- ROSS, A.N., S.B. VOSPER, 2005: Neutral turbulent flow over forested hills. – *Quart. J. Roy. Meteor. Soc.* **131**, 1841–1862, DOI: [10.1256/qj.04.129](https://doi.org/10.1256/qj.04.129).
- RUCK, B., E. ADAMS, 1991: Fluid mechanical aspects of the pollutant transport to coniferous trees. – *Bound.-Layer Meteor.* **56**, 163–195, DOI: [10.1007/BF00119966](https://doi.org/10.1007/BF00119966).
- SATHE, A., J. MANN, J. GOTTSCHALL, M.S. COURTNEY, 2011: Can wind lidars measure turbulence? – *J. Atmos. Ocean. Technol.* **28**, 853–868, DOI: [10.1175/JTECH-D-10-05004.1](https://doi.org/10.1175/JTECH-D-10-05004.1).
- SATHE, A., J. MANN, T. BARLAS, W. BIERBOOMS, G. VAN BUSSEL, 2013: Influence of atmospheric stability on wind turbine loads. – *Wind Energy* **16**, 1013–1032, DOI: [10.1002/we.1528](https://doi.org/10.1002/we.1528).
- SERAFIMOVICH, A., J. HÜBNER, M.Y. LECLERC, H.F. DUARTE, T. FOKEN, 2017: Influence of Low-Level Jets and Gravity Waves on Turbulent Fluxes. – Springer International Publishing, Cham, 247–276, DOI: [10.1007/978-3-319-49389-3_11](https://doi.org/10.1007/978-3-319-49389-3_11).
- SIYAL, S.H., U. MÖRTBERG, D. MENTIS, M. WELSCH, I. BABELON, M. HOWELLS, 2015: Wind energy assessment considering geographic and environmental restrictions in Sweden: A GIS-based approach. – *Energy* **83**, 447–461, DOI: [10.1016/j.energy.2015.02.044](https://doi.org/10.1016/j.energy.2015.02.044).
- SNYDER, W.H., R.S. THOMPSON, R.E. ESKRIDGE, R.E. LAWSON, I.P. CASTRO, J.T. LEE, J.C.R. HUNT, Y. OGAWA, 1985: The structure of strongly stratified flow over hills: dividing-streamline concept. – *J. Fluid Mech.* **152**, 249–288.
- SOGACHEV, A., J. MANN, E. DELLWIK, F. BINGÖL, O. RATHMANN, H. EJSING JØRGENSEN, O. PANFEROV, 2009: Wind energy availability above gaps in a forest. – In: *EWEC 2009 Proceedings*, volume 6, EWEC, 4198–4206.
- STEINFELD, G., S. RAASCH, T. MARKKANEN, 2008: Footprints in homogeneously and heterogeneously driven boundary layers derived from a lagrangian stochastic particle model embedded into large-eddy simulation. – *Bound.-Layer Meteor.* **129**, 225–248, DOI: [10.1007/s10546-008-9317-7](https://doi.org/10.1007/s10546-008-9317-7).
- STENSURD, D., 1996: Importance of low-level jets to climate: A review. – *J. Climate* **9**, 1698–1711, DOI: [10.1175/1520-0442\(1996\)009<1698:IOLLJT>2.0.CO;2](https://doi.org/10.1175/1520-0442(1996)009<1698:IOLLJT>2.0.CO;2).
- STIPERSKI, I., M.W. ROTACH, 2016: On the measurement of turbulence over complex mountainous terrain. – *Bound.-Layer Meteor.* **159**, 97–121, DOI: [10.1007/s10546-015-0103-z](https://doi.org/10.1007/s10546-015-0103-z).
- STOY, P.C., M. MAUDER, T. FOKEN, B. MARCOLLA, E. BOEGH, A. IBROM, M.A. ARAIN, A. ARNETH, M. AURELA, C. BERNHOFER, A. CESCATTI, E. DELLWIK, P. DUCE, D. GIANELLE, E. VAN GORSEL, G. KIELY, A. KNOHL, H. MARGOLIS, H. MCCAUGHEY, L. MERBOLD, L. MONTAGNANI, D. PAPALE, M. REICHSTEIN, M. SAUNDERS, P. SERRANO-ORTIZ, M. SOTTOCORNOLA, D. SPANO, F. VACCARI, A. VARLAGIN, 2013: A data-driven analysis of energy balance closure across fluxnet research sites: The role of landscape scale heterogeneity. – *Agricult. Forest Meteor.* **171-172**, 137–152, DOI: [10.1016/j.agrformet.2012.11.004](https://doi.org/10.1016/j.agrformet.2012.11.004).
- STULL, R.B., 1988: *An Introduction to Boundary Layer Meteorology*. – Springer Netherlands, Dordrecht.
- TAYLOR, P.A., 1987: Comments and further analysis on effective roughness lengths for use in numerical three-dimensional models. – *Bound.-Layer Meteor.* **39**, 403–418, DOI: [10.1007/BF00125144](https://doi.org/10.1007/BF00125144).
- TROEN, I., E. LUNDTANG PETERSEN, 1989: *European Wind Atlas*. – Risø National Laboratory.
- VESALA, T., N. KLJUN, U. RANNIK, J. RINNE, A. SOGACHEV, T. MARKKANEN, K. SABELFELD, T. FOKEN, M.Y. LECLERC, 2008: Flux and concentration footprint modelling: State of the art. – *Env. Pollution* **152**, 653–666, DOI: [10.1016/j.envpol.2007.06.070](https://doi.org/10.1016/j.envpol.2007.06.070).
- WHARTON, S., J.K. LUNDQUIST, 2012: Assessing atmospheric stability and its impacts on rotor-disk wind characteristics at an onshore wind-farm. – *Wind Energy* **15**, 525–546, DOI: [10.1002/we.483](https://doi.org/10.1002/we.483).
- WIERINGA, J., 1992: Updating the Davenport roughness classification. – *J. Wind Engin. Indust. Aerodyn.* **41**, 357–368.
- WILCZAK, J.M., S.P. ONCLEY, S.A. STAGE, 2001: Sonic anemometer tilt correction algorithms. – *Bound.-Layer Meteor.* **99**, 127–150, DOI: [10.1023/A:1018966204465](https://doi.org/10.1023/A:1018966204465).
- WILDMANN, N., S. BERNARD, J. BANGE, 2017: Measuring the local wind field at an escarpment using small remotely-piloted aircraft. – *Renewable Energy* **103**, 613–619, DOI: [10.1016/j.renene.2016.10.073](https://doi.org/10.1016/j.renene.2016.10.073).
- WOOD, N., 1995: The onset of separation in neutral, turbulent flow over hills. – *Bound.-Layer Meteor.* **76**, 137–164, DOI: [10.1007/BF00710894](https://doi.org/10.1007/BF00710894).
- ZERI, M., C. REBMANN, C. FEIGENWINTER, P. SEDLAK, 2010: Analysis of periods with strong and coherent CO₂ advection over a forested hill. – *Agricult. Forest Meteor.* **150**, 674–683, DOI: [10.1016/j.agrformet.2009.12.003](https://doi.org/10.1016/j.agrformet.2009.12.003).
- ZHANG, D.L., S. ZHANG, S.J. WEAVER, 2006: Low-level jets over the Mid-Atlantic States: Warm-season climatology and a case study. – *J. Appl. Meteor. Climatol.* **45**, 194–209, DOI: [10.1175/JAM2313.1](https://doi.org/10.1175/JAM2313.1).